Insect Biochemistry and Molecular Biology 58 (2015) 12–27

Contents lists available at ScienceDirect

Insect Biochemistry and Molecular Biology

journal homepage: www.elsevier.com/locate/ibmb

Molecular characterization and functional expression of the *Apis mellifera* voltage-dependent Ca^{2+} channels

Thierry Cens [a, b, c, *], Matthieu Rousset [a, b, c], Claude Collet [d], Mercedes Charreton [d], Lionel Garnery [e], Yves Le Conte [d], Mohamed Chahine [f], Jean-Christophe Sandoz [e], Pierre Charnet [a, b, c]

[a] Institut des Biomolécules Max Mousseron (IBMM), CNRS UMR 5247, Place Eugène Bataillon, 34095 Montpellier cedex 5, France
[b] Centre de Recherche de Biochimie Macromoléculaire (CRBM), CNRS UMR 5237, 1919 Route de Mende, 34293 Montpellier cedex 5, France
[c] Université de Montpellier, Place Eugène Bataillon, 34095 Montpellier cedex 5, France
[d] INRA UR 406 Abeilles et Environnement, 228 Route de l'aérodrome, Domaine Saint Paul, Site Agroparc, CS40509, 84914 Avignon cedex 9, France
[e] Laboratoire Evolution Génome et Spéciation (LEGS), CNRS UPR 9034, Avenue de la Terrasse, Bâtiment 13, 91198 Gif sur Yvette, France
[f] Centre de recherche, Institut universitaire en santé mentale de Québec, 2601 Chemin de la Canardière, Québec Québec G1J 2G3, Canada

ARTICLE INFO

Article history:
Received 9 December 2014
Received in revised form
9 January 2015
Accepted 9 January 2015
Available online 17 January 2015

Keywords:
Honeybee
Ca^{2+} channels
Cloning
Xenopus oocytes
Electrophysiology

ABSTRACT

Voltage-gated Ca^{2+} channels allow the influx of Ca^{2+} ions from the extracellular space upon membrane depolarization and thus serve as a transducer between membrane potential and cellular events initiated by Ca^{2+} transients. Most insects are predicted to possess three genes encoding Cavα, the main subunit of Ca^{2+} channels, and several genes encoding the two auxiliary subunits, Cavβ and Cavα2δ; however very few of these genes have been cloned so far. Here, we cloned three full-length cDNAs encoding the three Cavα subunits (AmelCav1a, AmelCav2a and AmelCav3a), a cDNA encoding a novel variant of the Cavβ subunit (AmelCavβc), and three full-length cDNAs encoding three Cavα2δ subunits (AmelCavα2δ1 to 3) of the honeybee *Apis mellifera*. We identified several alternative or mutually exclusive exons in the sequence of the AmelCav2 and AmelCav3 genes. Moreover, we detected a stretch of glutamine residues in the C-terminus of the AmelCav1 subunit that is reminiscent of the motif found in the human Cav2.1 subunit of patients with Spinocerebellar Ataxia type 6. All these subunits contain structural domains that have been identified as functionally important in their mammalian homologues. For the first time, we could express three insect Cavα subunits in *Xenopus* oocytes and we show that AmelCav1a, 2a and 3a form Ca^{2+} channels with distinctive properties. Notably, the co-expression of AmelCav1a or AmelCav2a with AmelCavβc and AmCavα2δ1 produces High Voltage-Activated Ca^{2+} channels. On the other hand, expression of AmelCav3a alone leads to Low Voltage-Activated Ca^{2+} channels.

1. Introduction

Ca^{2+} ions are a widespread second messenger that participates in many cellular functions. The flux of Ca^{2+} ions through Voltage-Gated Ca^{2+} Channels (VGCC) is involved in excitation-secretion coupling in neurons and endocrine cells, excitation-contraction coupling in muscular cells and excitation-transcription coupling (reviewed in Catterall, 2011; Bellis et al., 2013). In honeybees, Ca^{2+} influx participates in the formation and consolidation of the olfactory memory (see for review Sandoz, 2011). However, the precise role played by VGCCs in olfactory memory is difficult to evaluate without specific blockers. VGCCs open through plasma membrane depolarization, a process called activation, to allow the

Abbreviations: VGCC, Voltage-Gated Ca^{2+} Channel; HVA, High Voltage-Activated; LVA, Low Voltage-Activated; ORF, Open Reading Frame; RACE, Rapid Amplification of cDNA Ends; AID, Alpha Interaction Domain; GPI, glycosylphosphatidylinositol.

* Corresponding author. CRBM, UMR 5237, 1919 Route de Mende, 34293 Montpellier cedex 5, France. Tel.: +33 434359537; fax: +33 434359599.

E-mail addresses: thierry.cens@crbm.cnrs.fr (T. Cens), matthieu.rousset@crbm.cnrs.fr (M. Rousset), claude.collet@avignon.inra.fr (C. Collet), mercedes.charreton@avignon.inra.fr (M. Charreton), lionel.garnery@legs.cnrs-gif.fr (L. Garnery), yves.leconte@avignon.inra.fr (Y. Le Conte), mohamed.chahine@phc.ulaval.ca (M. Chahine), jean-christophe.sandoz@legs.cnrs-gif.fr (J.-C. Sandoz), pierre.charent@crbm.cnrs.fr (P. Charnet).

http://dx.doi.org/10.1016/j.ibmb.2015.01.005
0965-1748/

influx of ions from the extracellular space. Then, during persistent depolarization, they undergo inactivation and closure to prevent cytoplasmic Ca^{2+} overload. VGCCs are hetero-multimers composed of one Cavα subunit (the pore-forming subunit) that may be associated with auxiliary subunits, Cavβ and Cavα2δ (Fig. 1). The Cavα subunit carries most of the molecular apparatus that governs channel gating (opening and closure). The auxiliary subunits can profoundly modify channel gating and therefore deeply affect the properties of Ca^{2+} currents. Specifically, the Cavβ subunit increases Cavα sensitivity to voltage, thus hyperpolarizing the current–voltage curve, and speeds up or slows down channel inactivation (see for review Buraei and Yang, 2010). The Cavα2δ subunit also shapes the biophysical properties of Cavα, but less extensively than Cavβ (Dolphin, 2013). They both contribute to the trafficking and membrane stabilization of the channel (Felix et al., 2013). In mammals, where Ca^{2+} channels have been extensively studied, VGCCs are divided in two classes: Low Voltage-Activated (LVA) and High Voltage-Activated (HVA) channels that require low or high depolarization to open, respectively (Catterall, 2011). This phenotypic differentiation relies on the existence of different Cavα subunit families. Indeed, the Cav1 and Cav2 subunits give rise to HVA channels and the Cav3 subunits to LVA channels. Mammalian genomes contain four genes encoding four Cav1 subunits (Cav1.1 to 1.4), three genes encoding three Cav2 subunits (Cav2.1 to 2.3) and three genes encoding three Cav3 subunits (Cav3.1 to 3.3). These different Cavα subunits are structurally and functionally related, but have specific electrophysiological and pharmacological properties. Thus, Cav1 subunits give rise to L-type Ca^{2+} channels, Cav2 subunits to P/Q, N and R type Ca^{2+} channels, and Cav3 subunits to T-type Ca^{2+} channels (Catterall, 2011). While auxiliary subunits (Cavβ and Cavα2δ) are integral members of channel hetero-multimers formed with Cav1 or Cav2, there is little evidence for their association with Cav3. In mammals, there are four genes encoding Cavβ (Cavβ1 to 4) and four genes encoding Cavα2δ subunits (Cavα2δ1 to 4). As these auxiliary subunits finely tune Cavα properties, these multiple subunit combinations considerably increase the Ca^{2+} channel repertoire. Moreover, the presence of alternative exons in the coding sequence of all these subunits adds another layer of complexity. In invertebrates, including insects, things appear to be less complex because a single gene for the Cav1, Cav2 and Cav3 families has been identified and usually there is also a single gene for Cavβ, but several genes for Cavα2δ (Tyson and Snutch, 2013). Very few Ca^{2+} channel subunits have been cloned in invertebrates (Bouchard et al., 2006; Jeziorski et al., 1998; Kimura and Kubo, 2003, 2002; Kohn et al., 2001; Smith et al., 1998; Zheng et al., 1995) with the notable exception of the three Cavα and one Cavβ of the pond snail *Lymnaea stagnalis* (Dawson et al., 2014; Senatore and Spafford, 2010; Spafford et al., 2003, 2006). This is certainly explained by the difficulty to express invertebrate Cavα subunits in the heterologous expression systems commonly used for mammalian Ca^{2+} channels, such as *Xenopus* oocytes or *HEK293* cells (Salvador-Recatalà and Greenberg, 2012). Moreover, arthropod and mammalian Ca^{2+} currents display different pharmacological sensitivities and compounds commonly used in mammals to specifically discriminate the different types of Ca^{2+} channels cannot be easily used in insects (Jeziorski et al., 2000).

The genome of the honeybee *Apis mellifera* contains one gene for each Cavα family, a single gene for Cavβ and three genes for Cavα2δ (Weinstock et al., 2006). In a previous work, we reported the cloning of two Cavβ splice variants and their functional expression with a mammalian Cavα subunit (Cens et al., 2013). Here, we describe the molecular characterization of a third Cavβ splice variant, of the three Cavα and the three Cavα2δ subunits. We show that these subunits contain molecular domains that are functionally important for the electrophysiological properties of Ca^{2+} channels. We also describe for the first time the functional expression of insect VGCCs and demonstrate that the three Cavα subunits lead to distinctive Ca^{2+} currents. The heterologous expression of honeybee VGCCs will not only allow the characterization of the biophysical properties of these channels but also the assessment of specific blockers that would be used in intact honeybee cells.

2. Material and methods

2.1. Tissue preparation

Pupae and adult worker bees were anaesthetized by chilling at 4 °C. Heads, legs, abdomens, antenna were collected and stored on ice in TRIzol® Reagent (Life Technologies). Whole brain, mushroom bodies and antennal lobes were dissected rapidly under binocular microscope and stored on ice in TRIzol® Reagent.

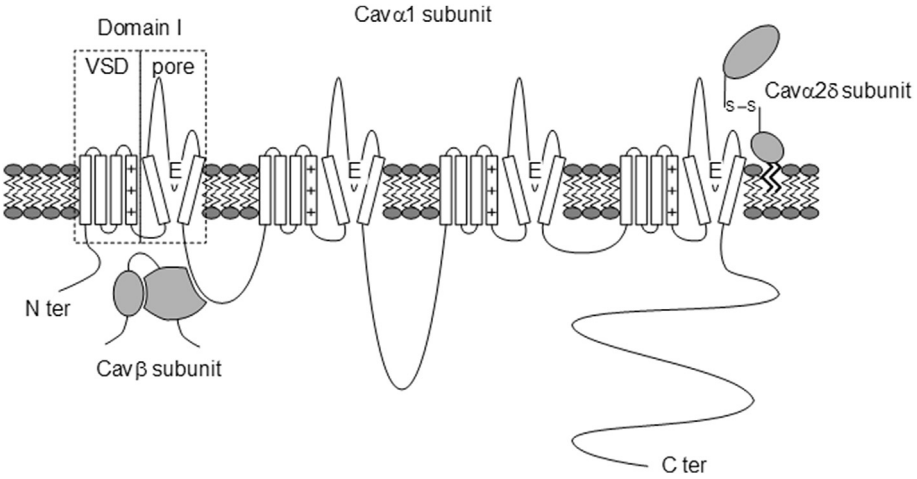

Fig. 1. Schematic representation of a voltage-gated Ca^{2+} channel. The Cavα1 subunit is composed of four domains (Domain I to IV) each containing six trans-membrane segments (S1–S6) and joined by linkers (the loops I-II, II-III and III-IV). The N- and C-terminus are cytoplasmic. Each domain can be divided in two functional units: the Voltage Sensor Domain (VSD), which includes the Arginine/Lysine-rich S4 segment (marked "+"), and the pore domain, which includes the P-loop with the selectivity filter (marked "E"). Cav1 and Cav2 subunits (not Cav3) are associated with auxiliary subunits: the cytoplasmic Cavβ subunit, which interacts with Cavα on the I-II loop, and the membrane-anchored Cavα2δ subunit.

2.2. Molecular biology

Total RNA was isolated from various tissues using TRIzol® Reagent according to the manufacturer's instructions. First-strand cDNA was obtained by reverse transcription of total RNA (1 μg from mushroom bodies or antennal lobes and 3 μg for the other tissues) using Oligo-dT primers and the Superscript II Reverse Transcriptase (Life Technologies) according to the manufacturer's instructions. PCR reactions were carried out with Herculase II Fusion Polymerase (Agilent Technologies). The 5′ end region of the different cDNAs was obtained by Rapid Amplification of cDNA Ends (RACE) PCR using the GeneRacer kit (Life Technologies). PCR fragments were gel-purified and cloned in the pBluescript-SK vector (Agilent technologies) for sequence analysis. Full length cDNAs were obtained by sequential ligation of the different PCR fragments using endogenous restriction sites. Fragments covering the entire Open Reading Frame (ORF) were finally cloned into the pcDNA3.1 (+) vector (Life Technologies). The Alfalfa Mosaic Virus (AMV) sequence was added immediately before the start codon and the 3′-UTR sequence of the *Xenopus* β−globin gene after the stop codon to boost expression in *Xenopus* oocytes (Venkatachalan et al., 2007). Vectors were linearized and cRNAs were *in vitro* transcribed using the T7 mMESSAGEmMACHINE kit (Life Technologies). Expression of the AmelCavα and AmelCavα2δ subunits during honeybee development and in various tissues from adult honeybees was assessed by RT-PCR analysis with the following primers: amcav1-031S (5′-GATTGGGCAAGTACTGCGATCCG-3′) and amcav1-012AS (5′-GAACACTAGAATCTATCGGCCGATGG-3′) to amplify nucleotides 5587-6015 of AmelCav1a (C-terminus); amcav2-003S (5′-GCTGCTCAGCTCGATGCGTAGC-3′) and amcav2-011AS (5′- CCTCCTCTTCCTCCTCGTTCTCGG-3′) to amplify nucleotides 1767-2149 of AmelCav2a (II-S5 and linker II-III); amcav3-006S (5′ CAACATTGAACCCTTGCAGCACTC-3′) and amcav3-013AS (5′-AAGAGAATTGGCCGCAGAGCA-3′) to amplify nucleotides 6828-7512 of AmelCav3a (C-terminus); primers amcava2d-027S (5′- TAGTCTACCAGAACATGACCACACCG-3′) and amcava2d-015AS (5′-CAAACCACTGGGTTACCTTCGCA-3′) to amplify nucleotides 2068-2474 of AmelCavα2δ1 (3′ end of the α2 peptide); amcava2d-030S (5′-TTCCGACAAAACTACGAGTCAGATCC-3′) and amcava2d-021AS (5′-TTGCAATAGTTTTTCCCATGCCTG-3′) to amplify nucleotides 711-1035 of AmelCavaα2δ2 (5′ end of the α2 peptide); and amcava2d-006S (5′-ATCCTCGACACGTTAGGCCCG-3′) and amcava2d-002AS (5′-TGGATGTAATGGGCCGTCGTATTC-3′) to amplify nucleotides 1066-1938 of AmelCavaα2δ3 (VWA and Cache domains). Sequence alignment and amino acid sequence homologies between the honeybee and human subunits were determined with the Vector NTI program (Life Technologies).

2.3. Xenopus oocytes preparation and injection

Preparation of *Xenopus* oocytes was previously described (Cens et al., 1996). Mixtures of different cRNAs (1 μg/μl for each AmelCavα ± AmelCavβ ± AmelCavα2δ; mol:mol:mol) were injected as previously described (Cens et al., 1996). About 30 *Xenopus* oocytes were injected with 1 μl of solution.

2.4. Electrophysiological recordings and current analysis

Ba^{2+} currents were recorded as previously described (Cens et al., 2013). Current−voltage curves were fitted using the following equation:

$$I/Imax = G^*(V - Erev)/(1 - \exp((V - Va)/ka))$$

where I is the current amplitude measured during depolarization V (from −80 to +50 mV); $Imax$ is the peak current amplitude measured at the maximum of the current−voltage curve; G is the normalized macroscopic conductance, $Erev$ is the apparent extrapolated reversal potential, Va is the potential for half activation, and ka is a slope factor.

3. Results and discussion

3.1. Molecular cloning of three honey bee Cavα subunits

To clone the cDNAs encoding the three honeybee Cavα subunits, we employed conventional RT-PCR strategy using total RNA from whole adult heads and primers based on the predicted cDNA sequences (Amel_1.0, Weinstock et al., 2006) to amplify the coding sequences up to the 3′ end. To obtain the 5′ ends we used a RACE protocol. Despite numerous attempts, we could not amplify the complete Open Reading Frame (ORF) of each Cavα subunit in a single PCR reaction, and we produced the complete cDNAs by ligation of overlapping PCR fragments. This strategy allowed us to identify several splice variants in the sequence of AmelCav2 and two mutually exclusive exons in the sequence of AmelCav3, but none in AmelCav1. However, future experiments may reveal also AmelCav1 variants and additional variants for the AmelCav2 and AmelCav3 subunits as suggested by the last release (Amel_4.5) of the *A. mellifera* genome assembly (Elsik et al., 2014).

3.1.1. The Cav1 subunit

The AmelCav1a genomic sequence contains 41 exons that are predicted to span 29 kb (Supplementary Fig. 1). The AmelCav1a cDNA (deposited in Genbank: KJ485704 [1]) contains an ORF of 5934 bp encoding a protein of 1978 amino acids (Fig. 2). We found that exons 1 and 21 contained nucleotides that had not been identified in the genome assembly (neither the Amel1.0 nor the Amel4.5 release). This partially explains the differences between the AmelCav1a and the predicted Cav1 sequence (Genbank: XM_003251258.1 that has been removed and replaced by a new version XM_006569121.1 since the beginning of this study). The sequence of exon 1, which we obtained by RACE, is missing in the latest prediction of the Cav1 sequence. However, the deduced amino acid sequence of AmelCav1a N-terminus is very similar to that of the predicted Cav1 subunits in other arthropod species, for examples *Bombus terrestris* or *Harpegnathos saltator* (Genbank: XP_003393703 and EFN84355, respectively, not shown). Exon 21 encodes the trans-membrane segments S2 and S3 of domain III (IIIS2 and IIIS3, see Fig. 1) of the Cavα subunit. The AmelCav1a C-terminus contains a stretch of glutamine reminiscent of a polyglutamine tract (polyQ, Fig. 2). In mammals, polyQ sequences are found in many proteins (Butland et al., 2007) and in humans, polyQ motifs with a number of glutamines that exceeds a certain threshold have been implicated in severe neurodegenerative diseases (Gatchel and Zoghbi, 2005; Williams and Paulson, 2008). Spinocerebellar Ataxia Type 6 is caused by an abnormally long (>20 glutamines) polyQ tract in the C-terminus of the Cav2.1 Ca^{2+} channel subunit. To determine whether in honeybees, like in humans, the polyQ length in AmelCav1a is variable, we collected

[1] The sequences deposited in the Genbank under the number KJ485704−KJ485709 and JX997993 are patented (patent # FR 3003863/WO 2014155021).

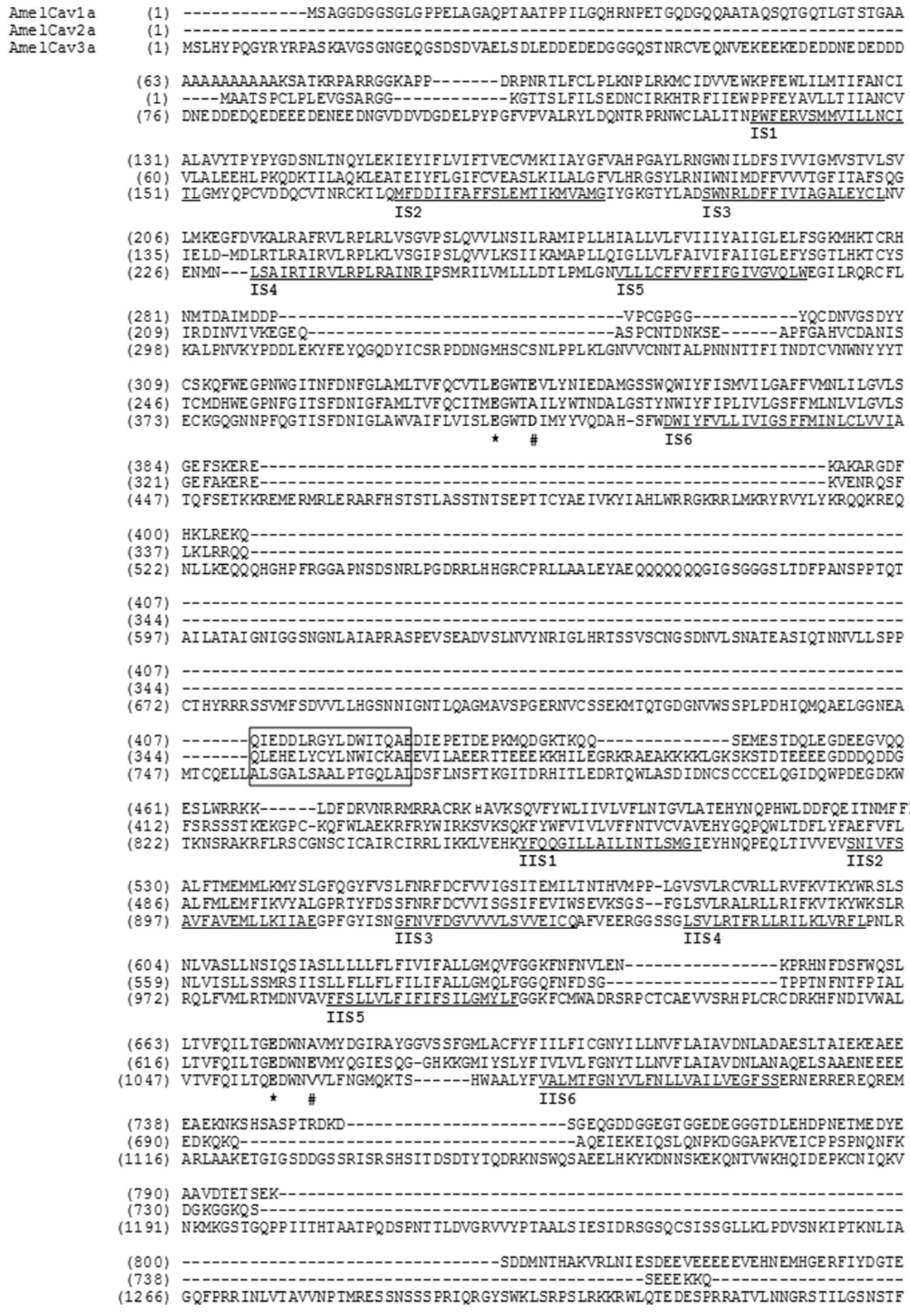

Fig. 2. Alignment of the AmelCavα subunit amino acid sequences. Dashes represent gaps introduced to maximize sequence alignment. The six trans-membrane segments (S1–S6) of each domain (I to IV) are indicated under the sequences. The amino acids that define the AmelCav1a and AmelCav2a Alpha Interacting Domain (AID) involved in Cavα–Cavβ interaction are boxed. The EEEE and DCS loci, important for selectivity and conductance, are marked by * and #, respectively, in each domain. The polyQ tract in the AmelCav1a C-terminus is highlighted in bold. Sequences were deposited in Genbank under accession numbers KJ485704–KJ485706.

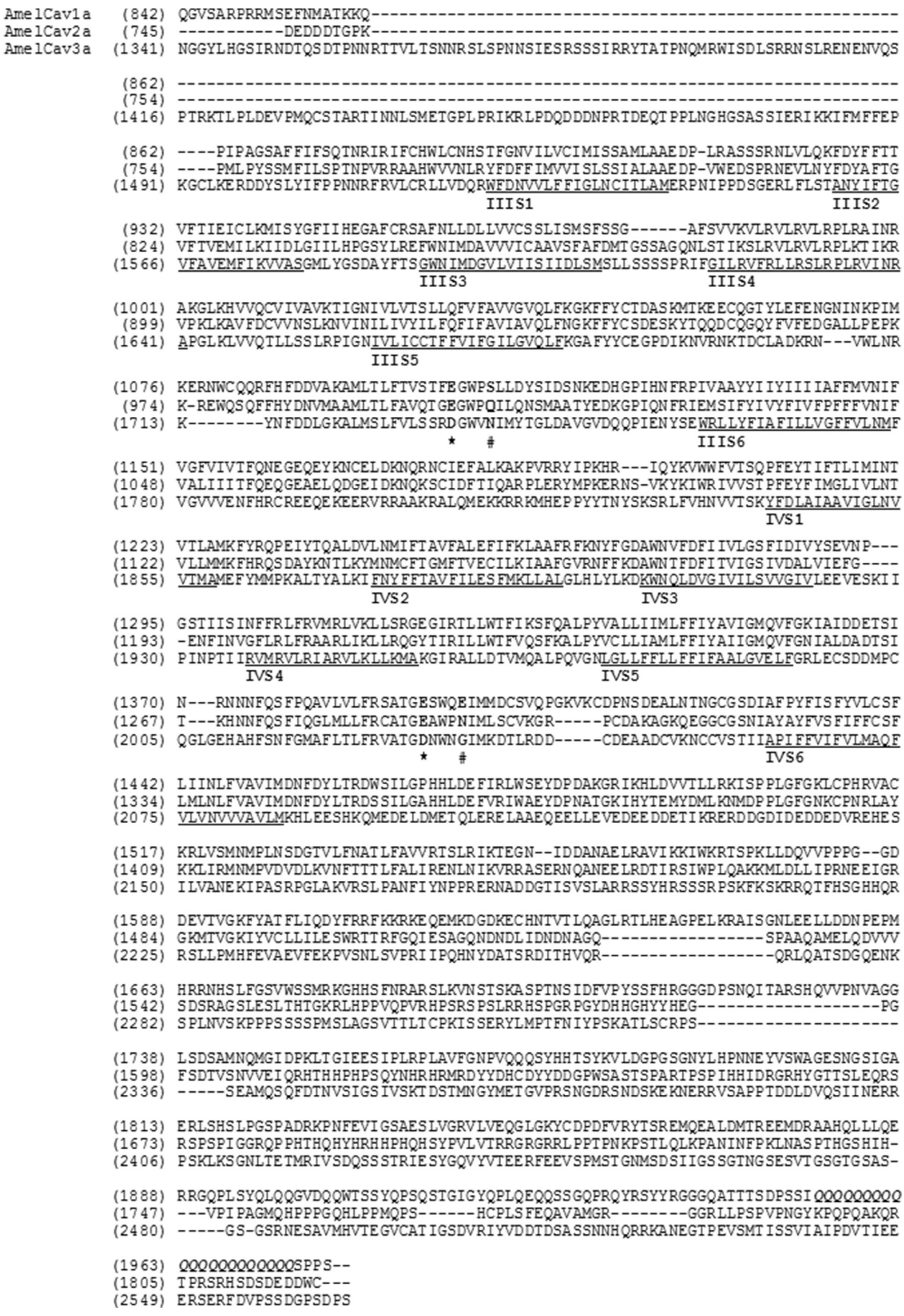

Fig. 2. (*continued*).

Table 1
Analysis of AmelCav1 C-terminal sequence in DNA isolated from honeybees collected in different countries.

Country	City	Sequence	Number of Gln	n
France	Rochefort	GGQ**A**TTTSDP**S**SIQQQQQQQQQQQQQQQQQQQQQQQ----SPPS	21	2
		.....QQQQQQQQQQQQQQQQQQQQQQQ---....	22	
	St Mathieu de Tréviers	.....QQQQQQQQQQQQQQQQQQQ-------....	18	4
		.....QQQQQQQQQQQQQQQQQQQQQQQ----....	21	
		.....QQQQQQQQQQQQQQQQQQQ-------....	18	1
		.....QQQQQQQQQQQQQQQQQQQQQQQ---....	22	
		.....QQQQQQQQQQQQQQQQQQQQQQQ----....	21	1
		.....QQQQQQQQQQQQQQQQQQQQQQQ----....	21	
	Avignon	.....QQQQQQQQQQQQQQQQQQQQQQQ----....	21	1
		.....QQQQQQQQQQQQQQQQQQQQQQQQ-....	24	
		.....QQQQQQQQQQQQQQQQQQQQQQQ----....	21	1
		.....QQQQQQQQQQQQQQQQQQQQQQQQQ....	25	
		.....QQQQQQQQQQQQQQQQQQQQQQQ---....	22	1
		.....QQQQQQQQQQQQQQQQQQQQQQQQQ....	25	
		.....QQQQQQQQQQQQQQQQQQ------....	19	1
		...**T**.....**T**..QQQQQQQQQQQQQQQQQQQQQQQQQ....	25	
Turkey	Eskischir	...**T**.....**T**..QQQQQQQQQQQQQQQQQQ------....	19	2
		.....QQQQQQQQQQQQQQQQQQQQQQQ----....	21	
Algeria	Boufarik	.....QQQQQQQQQQQQQQQQQQQQQQQ----....	21	1
		.....QQQQQQQQQQQQQQQQQQQQQQQ---....	22	
		.....QQQQQQQQQQQQQQQQQQQQQQQ---....	22	1
		.....QQQQQQQQQQQQQQQQQQQQQQQ---....	22	
Bulgaria	Birimirzi	.....QQQQQQQQQQQQQQQQQQQQQQQ----....	21	2
		.....QQQQQQQQQQQQQQQQQQQQQQQ----....	21	

Dots represent identical amino acids and dashes gaps in the alignment.

specimens (n = 18) from different locations in France, Algeria, Turkey and Bulgaria (Table 1). We found that they were mostly (14/18) heterozygous and that the number of glutamines residues in the polyQ motif varied between 18 and 25. Although this seems very limited compared to humans, where it may range from 7 to 16 in healthy individuals (Butland et al., 2007), we cannot exclude that by increasing the sample size we may detect a larger polyQ length variability also in honeybees. A BLAST analysis using the AmelCav1a C-terminus showed that the polyQ tract was absent in the otherwise very similar *B. terrestris* and *Bombus impatiens* Cav1 sequences (Genbank: XP_003393703 and XP_003490120, respectively), but present in the *Apis florea* and *Apis dorsata* Cav1 sequences (Genbank: XP_003697046 and XP_006618300, respectively). This suggests that the presence of a polyQ tract in Cav1 is specific to the *Apis* genus. Moreover, it is quite surprising to find a polyQ of "pathological" length (up to 25 glutamine residues) in the C-terminus of honeybee Cav1, but this could help understanding the consequences of its presence in human Ca^{2+} channels.

3.1.2. The Cav2 subunit

Cav2 genomic sequence contains 34 exons, the shortest (exon 29) leading to the addition of only three amino acids, that are predicted to span 77 kb (Supplementary Fig. 1). The AmelCav2a cDNA (deposited in Genbank: KJ485705) contains an ORF of 5460 bp encoding a protein of 1819 amino acids (Fig. 2). The predicted cDNA for the Cav2 subunit available at the beginning of this work (Genbank: XM_392298) lacked exons 27 and 32, and differed from AmelCav2a at the N-terminus and at the junctions between exons 10 and 11, 13 and 14 and 33 and 34. The differences observed at the junctions were not present in the new assembly of the honeybee genome (Amel_4.5) that also confirmed the presence of the exons 27 and 32. The single remaining difference concerns the AmelCav2a N-terminus which is not found in any of the predicted Cav2 isoforms. Moreover, we could not amplify, using specific primers, the long 5′ end of Cav2 that is present in the outdated (Genbank: XM_392298) and also in the new version (Genbank: XM_006557941) of the predicted Cav2 sequence. We identified by RACE another N-terminus resulting from the alternative joining of exons 2 and 3 (not shown). This alternative N-terminus is present in some isoforms of the predicted Cav2 (Genbank: XM_006557953 and XM_006557954). Exons 20, 27, 28, 29 and 32 are alternatively spliced, whereas exon 23a and 23b are mutually exclusive (Supplementary Fig. 1). The insertion of exon 20 adds 16 amino acids to the S3–S4 linker of Domain IV (Fig. 3A). Interestingly, the insertion of an alternative exon encoding only two amino acids at a similar position in the mammalian Cav2.1 subunit strikingly modifies the channel sensitivity to inhibition by the toxin ω-Aga-IVA (Bourinet et al., 1999; Hans et al., 1999). It is, therefore, tempting to speculate that the insertion of exon 20 might modify the pharmacology of the honeybee Cav2 channel. This additional sequence may also affect the sensitivity of the channel to transmembrane voltage and/or to external ions. Indeed, specific amino acids similarly located in the S3–S4 linker of the mammalian Cav3.2 and Cav2.3 subunits are involved in the channel sensitivity to extracellular Ni^{2+} or H^{+}, respectively (Cens et al., 2011; Kang et al., 2006). Exon 23 encodes the beginning of

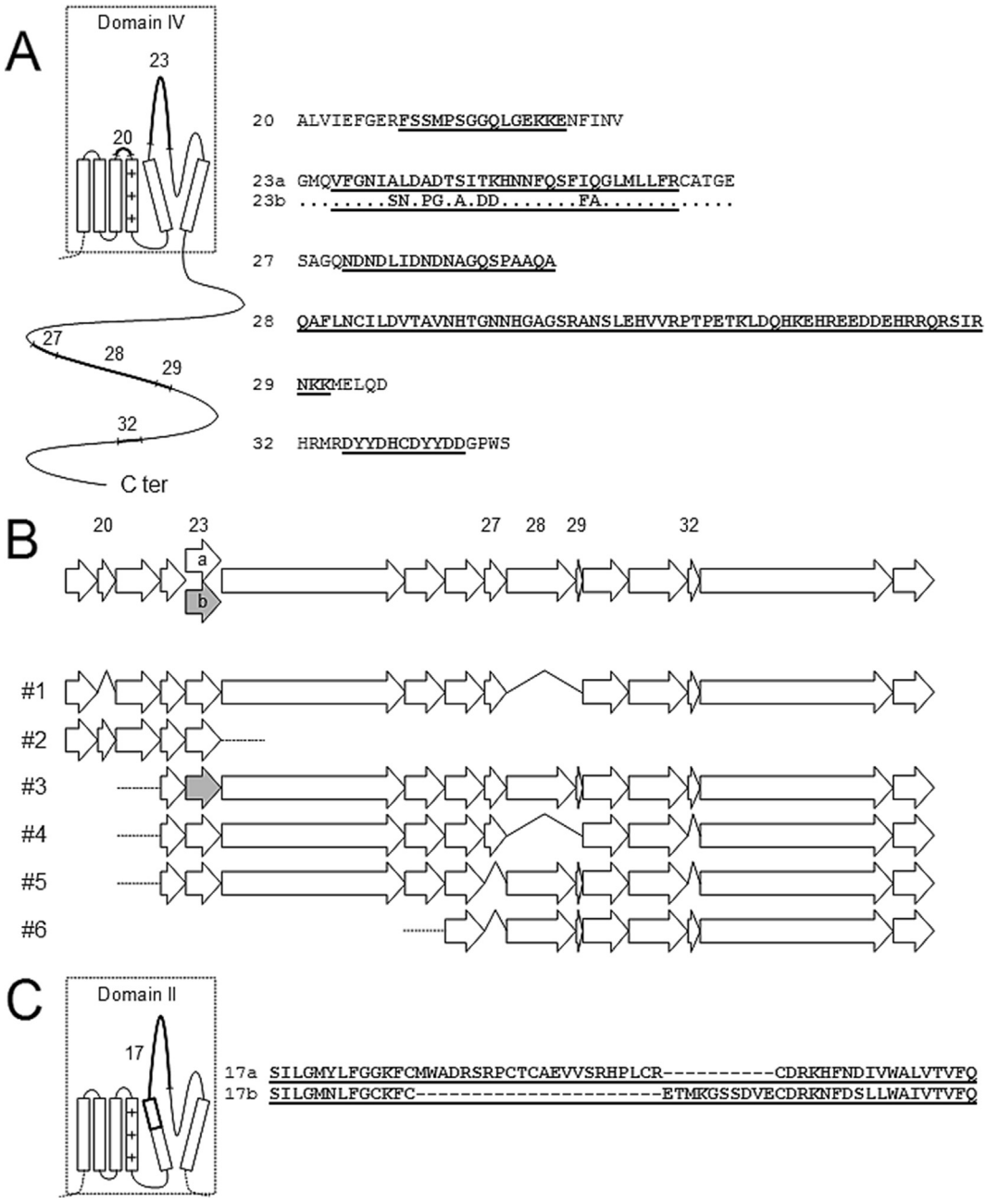

Fig. 3. Alternative and mutually exclusive exons of the AmelCav2 and AmelCav3 subunits. **A**. Schematic representation of Domain IV of the AmelCav2 subunit and location of the alternative exons 20, 27, 28, 29 and 32 and of the mutually exclusive exons 23a and 23b with their respective amino acid sequences (bold and underlined). Dots represent similar amino acids. **B**. Combination of coding exons in six independent PCR fragments of AmelCav2 (#1 to #6: sequences were deposited in Genbank under the accession numbers KM577626%5fKM577631). **C**. Schematic representation of AmelCav3 Domain II and location of the mutually exclusive exons 17a and 17b with their respective amino acid sequences. Dashes represent gaps in the amino acid sequences. The sequence of the fragment including exon 17b has been deposited in Genbank (accession number KM577632).

the S5–S6 linker of Domain IV (Fig. 3A). Exon 23a differs from exon 23b by only nine amino acids, but this difference could influence the channel conductance because these residues are located in the outer mouth of the channel pore (Cens et al., 2011). Exons 27, 28, 29 and 32 are located in the C-terminus (Fig. 3A) that, in mammalian Cav1 and Cav2, contains several domains that can modify the channel biophysical properties, such as Ca^{2+}-dependent facilitation and Ca^{2+}-dependent inactivation (Cens et al., 2006) or the regulation of these properties by Ca^{2+} binding proteins (Lee et al., 2002). With the exception of exons 28 and 29, which were always found together, the exons of AmelCav2 C-terminus seem to be expressed in multiple combinations (Fig. 3B). This considerably increases the number of Cavα subunits that may harbor specific properties.

3.1.3. The Cav3 subunit

The genomic sequence of AmelCav3 contains 36 exons that are predicted to span 190 kb (Supplementary Fig. 1). Exons 17a

and 17b are mutually exclusive. AmelCav3a cDNA (Genbank: KJ485706) contains an ORF of 7698 bp encoding a protein of 2566 amino acids (Fig. 2). Probably because of the poor quality of the genomic sequence, there was no predicted full length Cav3 subunit in the honeybee genome, when we started this study, but only a partial sequence (Genbank: XM_624269). Indeed, exons 5, 10, 19, 22 and 26 of AmelCav3 contain nucleotides that were not identified in the first assembly of the honeybee genome (Amel_1.0). Nevertheless, AmelCav3a sequence is close to the predicted Cav3 sequence in other arthropod species, such as *A. florea* (Genbank: XP_003698162). The last assembly of the honeybee genome (Amel_4.5) contains a predicted cDNA for the Cav3 subunit (Genbank: XM_006562038) that is very close to that of AmelCav3a. Exons 17a and 17b encode a 53 or 41 amino acid-long fragment in the S5–S6 linker of Domain II (Fig. 3C). As described for exon 21 of AmelCav2, this exchange could influence the conductance of the honeybee Cav3 channel. Moreover, like in mammals, where it plays a critical role in Cav3 channel trafficking and gating (Vitko et al., 2007), the I-II linker is much longer in AmelCav3a than in the other two Cavα subunits (Fig. 2). It also contains a glutamine stretch that is shorter than the polyQ tract found in AmelCav1a C-terminus. However, we found an extra glutamine in a PCR fragment encompassing the same sequence, suggesting that this "polyQ" motif, like that of AmelCav1, is subject to length variability (not shown).

3.2. Comparison of the honeybee and the human Cavα subunits

The degree of homology between honeybee Cavα subunits was comparable to that found between human Cavα subunits (Supplementary Table 1). Moreover, when we specifically compared the three Cav1, Cav2 or Cav3 families, none of the honeybee Cavα subunits showed a particularly high homology with a specific human subunit (Supplementary Table 1). As expected, the homology between honeybee and human Cavα subunits was particularly important within the Domains (Fig. 4) whereas the connecting linkers and the N- and the C-terminus differed substantially. However, the AmelCav1a proximal C-terminus, which contains the pre-IQ and IQ domains that are involved in the interaction with the Ca^{2+} binding protein calmodulin and are therefore important for the Ca^{2+}-dependent regulation of channel properties (Cens et al., 2006), presented a strong homology with its mammalian counterpart, like in other invertebrates (Taiakina et al., 2013). This suggests that such regulation may also exist in honeybee Ca^{2+} channels.

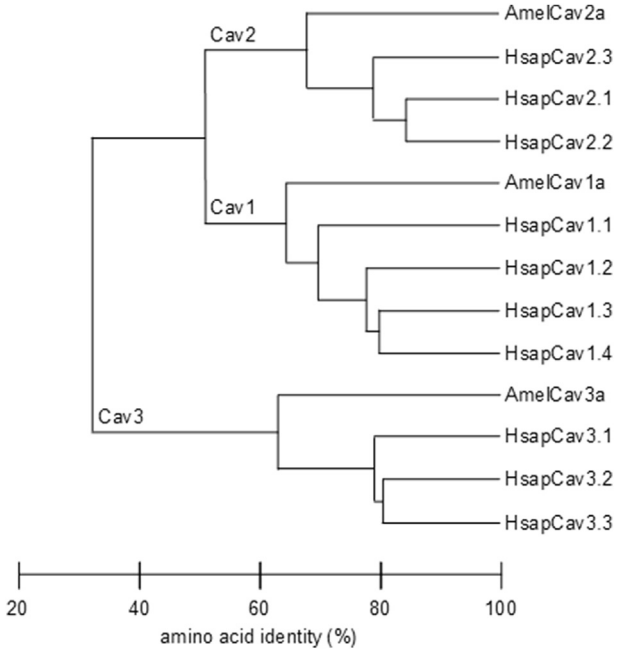

Fig. 4. Dendrogram illustrating the similarity of the honeybee and human Cavα subunits. The dendrogram was drawn using the Phylogeny platform (Dereeper et al., 2008) (www.phylogeny.fr) and MUSCLE3.6 and PhyML3.0 and the following human sequences: Cav1.1 (AAA51902), Cav1.2 (AAA51900), Cav1.3 (NP_000711), Cav1.4 (CAA12175), Cav2.1 (AAB64179), Cav2.2 (AAA51897), Cav2.3 (AAA72125), Cav3.1 (AAD29401), Cav3.2 (NP_066921) and Cav3.3 (AAF44626). Only the sequences of the domains I to IV were used for this analysis.

3.2.1. The S4 segments

Fig. 5 displays an alignment of the S4 segments of each Domain (IS4 to IVS4) of the honeybee and human Cavα subunits. The presence of regularly spaced basic amino acids (arginine or lysine) allows the S4 segments to play the role of voltage-sensors that move through the membrane in response to modifications of the membrane potential. Various mechanisms (reviewed in Tombola et al., 2006; Bezanilla, 2008) have been proposed to explain the coupling between S4 movement and channel opening. Although it would be highly speculative to favor one mechanism rather than another, it is worth noting the high conservation of the S4 segment sequences in the honeybee and human Cavα subunits. This suggests a relative similarity of the voltage-dependent properties of these channels in agreement with Ca^{2+} current recordings realized in honeybee neurons and muscle cells (Collet, 2009; Kloppenburg et al., 1999; Laurent et al., 2002; Schäfer et al., 1994). However, the lack of specific blockers/markers did not allow concluding whether the recorded currents resulted from the activity of a single or several types of Ca^{2+} channels. The presence of LVA Ca^{2+} channels in honeybee tissues has not been unambiguously reported yet. However, the hump in some current–voltage curves that appeared at low voltage suggests the existence of such Ca^{2+} channels in honeybee muscle cells (Cens et al., 2013). It has recently been shown that the Cav2 subunit may produce both HVA and LVA Ca^{2+} currents in *Drosophila* (Ryglewski et al., 2012). In fact, only the expression of an insect Cav3 subunit, which has never been done so far, would undoubtedly prove that AmelCav3 form an LVA Ca^{2+} channel (see below).

3.2.2. The selectivity filter

The most outstanding property of voltage-gated Ca^{2+} channels is probably their remarkable specificity for Ca^{2+} ions. The ion-conducting pore is composed by the four S5, the four P-loops and the four pore-lining S6. The selectivity towards divalent cations is achieved by four negatively charged amino acids (glutamate or aspartate) that delimit the EEEE locus, a Ca^{2+}-binding site located in the narrowest part of the channel pore. This locus is composed of one glutamate from each of the four P-loops of Cav1 and Cav2 subunits (EEEE). Conversely, in the Cav3 subunit, the P-loops of the first two domains contain a glutamate and the P-loops of the last two domains contain an aspartate (EEDD). Mutations at this site severely affect the Ca^{2+} channel selectivity and/or permeability (reviewed in Sather and McCleskey, 2003). The EEEE locus constitutes the molecular signature for voltage-gated Ca^{2+} channels and was perfectly conserved in the honeybee Cavα subunits as well (Fig. 6). Besides the EEEE locus, another ring of charged and non-charged amino acids, the DCS locus (for Divalent Cation Selectivity), is responsible for the specific permeation profiles of Ca^{2+} channels

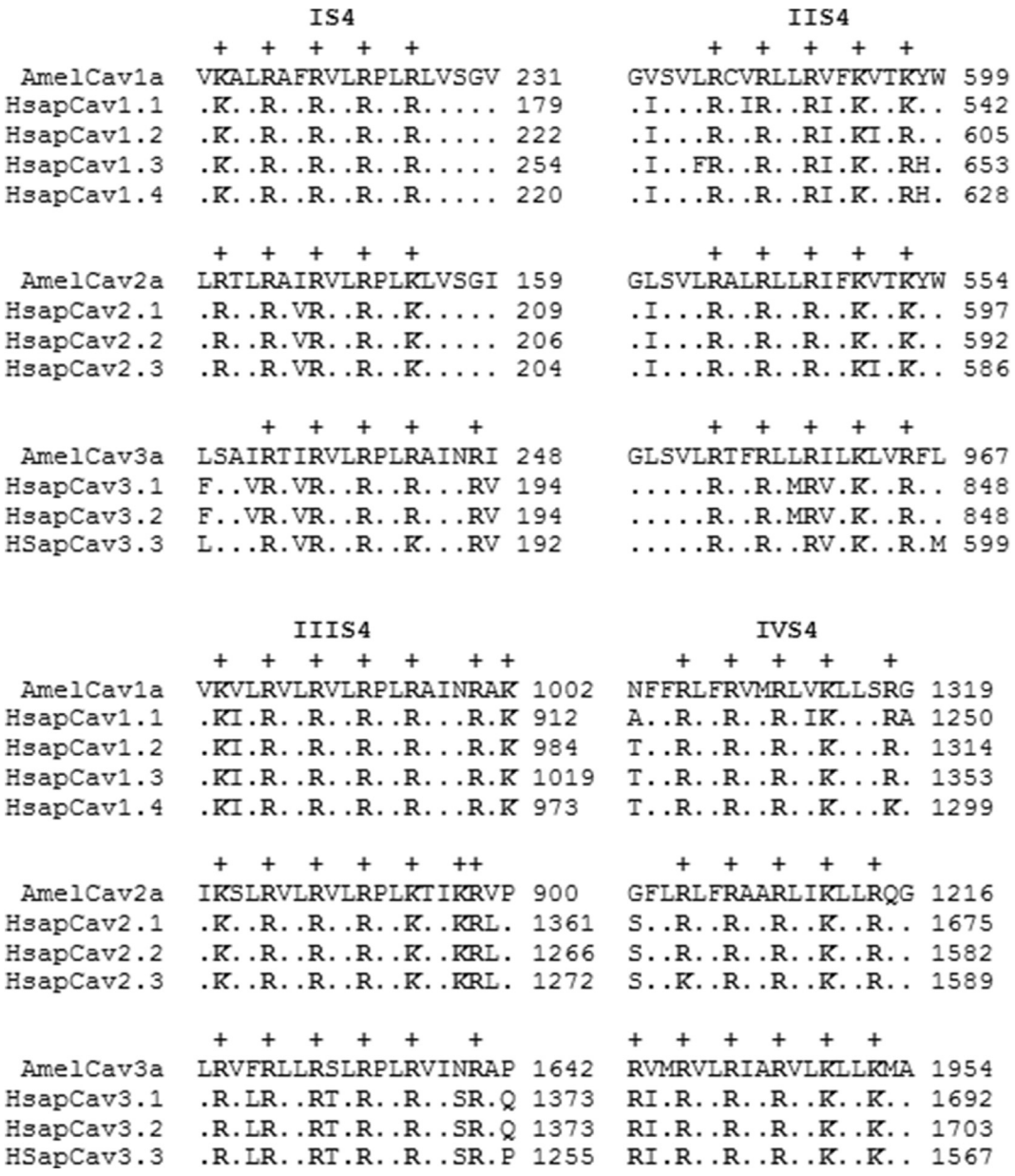

Fig. 5. Alignment of the S4 segments of the honeybee and human Cavα subunits. The human sequences used for this alignment are the same as in Fig. 4. The charged amino acids (arginine/lysine) are marked by the plus sign. Dots represent identical amino acids.

towards divalent cations (Cens et al., 2007). Both the number of charged amino acids and their relative position in the DCS locus define the channel permeation profile. AmelCav1a DCS locus was similar to the DCS locus of mammalian Cav1.1, 1.3 and 1.4, as it had two charged amino acids and the DCS locus of AmelCav3a to that of Cav3.3. By contrast, AmelCa2a DCS locus had only one charged amino acid and thus, was clearly different to that of the three mammalian Cav2 subunits (Fig. 6).

3.3. Molecular cloning of a new variant of the honey bee Cavβ subunit

We previously reported the cloning and functional expression of two variants of the honeybee Cavβ subunit and the role played by their different N-terminal sequences in the specific regulation of channel inactivation when co-expressed with a mammalian Cavα subunit (Cens et al., 2013). Mammalian genomes contain four genes that encode four distinct Cavβ subunits, which are composed of two conserved domains (C1 and C2) flanked and joined by more variable regions (V1, V2 and V3, see Fig. 7A). C1 and C2 were predicted by crystallographic modeling to contain a *src* homology 3 (SH3) domain and a guanylate kinase-like (GK) domain, an association that characterizes the MAGUK family of scaffolding proteins (Chen et al., 2004; Hanlon et al., 1999; Opatowsky et al., 2004; Van Petegem et al., 2004). The SH3 domain is split by an intervening sequence of variable length (the HOOK domain) that connects C1 and C2 (Fig. 7A). The GK domain binds tightly to the I-II loop of the Cavα subunit through the alpha-interaction domain (AID, see Fig. 1) and is involved in intramolecular coupling with the SH3 domain (reviewed in

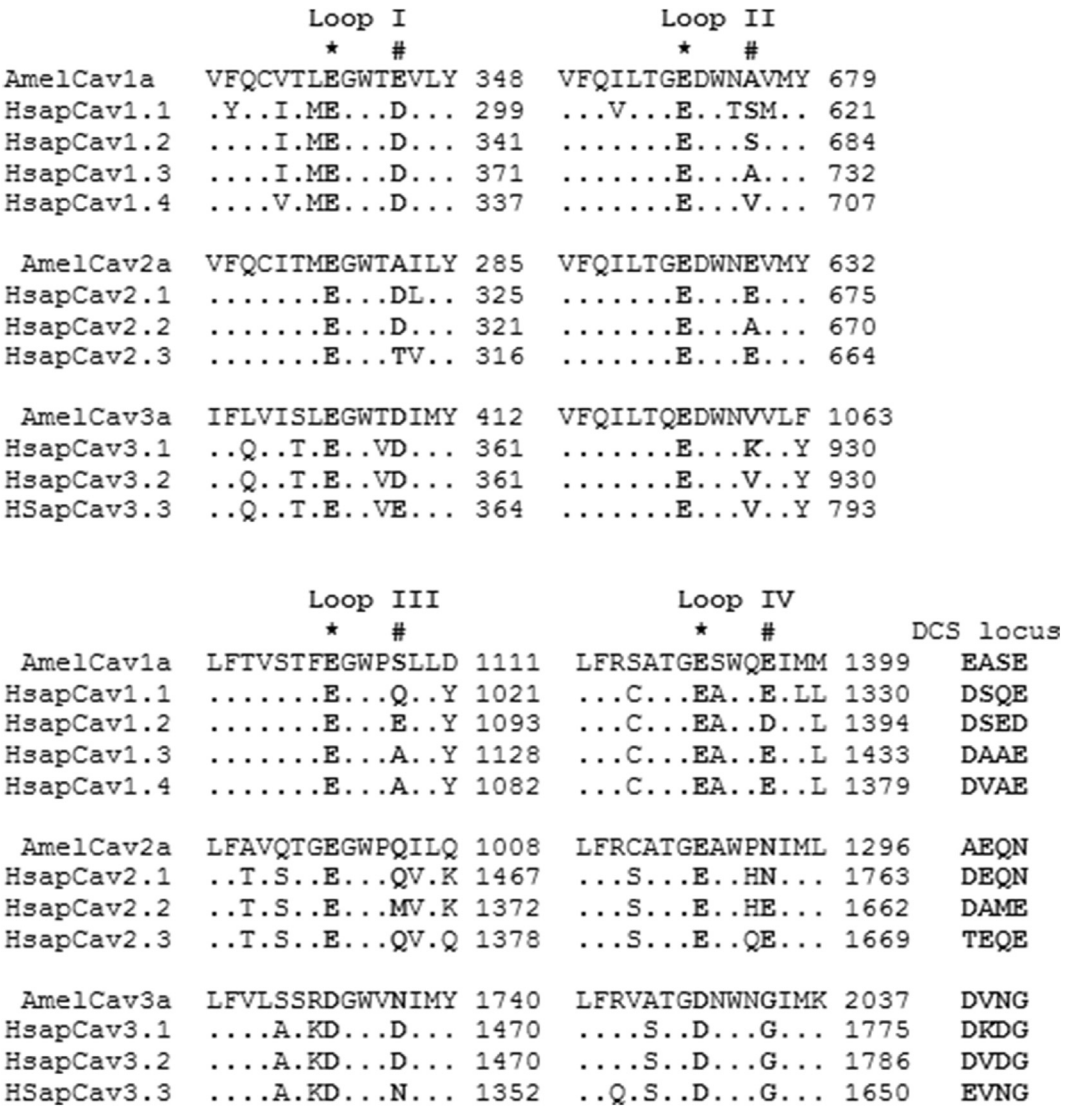

Fig. 6. Alignment of the P-loops of honeybee and human Cavα subunits. The human sequences used for this alignment are the same as in Fig. 4. The amino acids of the EEEE (*) and the DCS (#) loci are highlighted in bold. The sequence of the DCS locus of each Cavα subunit is shown at the bottom on the right. Dots represent identical amino acids.

Buraei and Yang, 2010). The GK-AID interaction is sufficient to allow Cavα membrane trafficking and, consequently, for increasing current amplitude. The GK-SH3 interaction is important for the specific gating regulations provided by the different Cavβ subunits. In particular, the HOOK domain and the N-terminus play a predominant role in modulating channel inactivation (Cens et al., 1999; He et al., 2007; Miranda-Laferte et al., 2012; Olcese et al., 1994; Qin et al., 1996; Restituito et al., 2000; Richards et al., 2007). The sequences of these two regions are extensively spliced in the mammalian Cavβ subunits (Buraei and Yang, 2010). Here, we clone AmelCaβc (Genbank: JX997993), a third variant of the honeybee Cavβ subunit that shares exon 1a with AmelCavβa but lacks exon 9, like AmelCavβb (Supplementary Fig. 2). Compared to AmelCavβa and AmelCavβb, AmelCavβc has a longer exon4 that adds 12 amino acids to the HOOK domain through the use of an alternative donor site (Fig 7B). Mutually exclusive splicing of exon 7 of the mammalian Cavβ1 and Cavβ2 subunits spanning the 3′ end of the HOOK domain leads to a V2 sequence of variable length because exon 7a adds 44 amino acids, including a polybasic domain also found in honeybee Cavβ (Cens et al., 2013), while exon7b adds only 6 amino acids (Buraei and Yang, 2010). In *L. stagnalis*, exon 7, spanning the HOOK domain, can be skipped altogether or, via the use of an alternative acceptor site, can lead to a V2 sequence containing seven extra amino acids (Dawson et al., 2014). In *A. mellifera*, like in mammals (He et al., 2007; Richards et al., 2007) and snails (Dawson et al., 2014), the HOOK domain may work together with the N-terminus to regulate channel inactivation. The availability of the whole repertoire of Ca^{2+} channel subunits will undoubtedly be an asset to assess the functional consequences of Cavβ alternative splicing on the various honeybee Ca^{2+} channels.

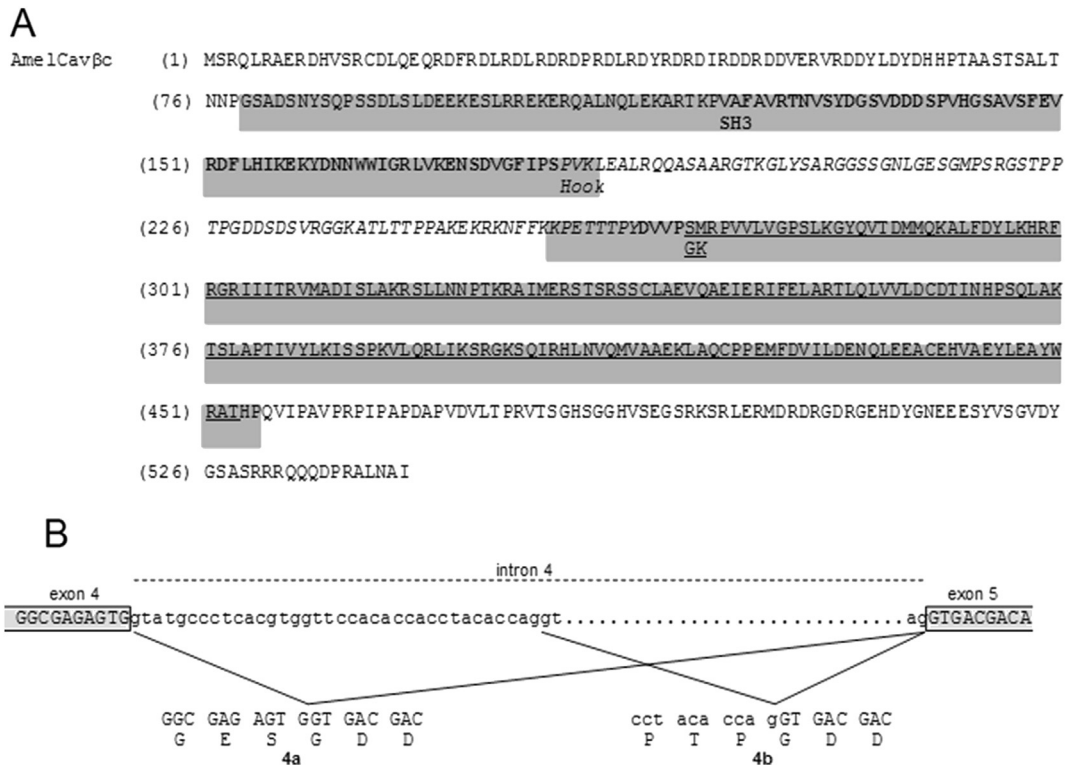

Fig. 7. Amino acid sequence of the AmelCavβc subunit. A. The two conserved C1 and C2 domains are highlighted in light gray, the SH3 in **bold**, the HOOK in *italic* and the GK sequence is underlined. B. Schematic representation of the alternative use of the donor site at the junction between exons 4 and 5 of AmelCavβc, based on the Genbank genomic sequence NC_007082.3. The AmelCavβc sequence was deposited in Genbank (accession number JX997993).

3.4. Molecular cloning of the three honey bee Cavα2δ subunits

The mammalian genome contains four genes encoding four different Cavα2δ subunits. Cavα2δ subunits are post-translationally cleaved to produce an extracellular, heavily glycosylated, α2 peptide and a membrane-associated δ peptide. These two peptides are linked through a disulfide bond (see for review Dolphin, 2013). The site of the proteolytic cleavage has been identified only in the Cavα2δ1 subunit, but the involved protease remains unknown (Andrade et al., 2007). Similarly, the cysteine residues that participate in the formation of the disulfide bond have been recently identified in the sequence of mammalian Cavα2δ1 (Calderón-Rivera et al., 2012), but other cysteine residues could be involved in the other Cavα2δ subunits. Moreover, little is known on how Cavα2δ affects channel properties, because the interaction between Cavα1 and Cavα2δ has only been partially unraveled (Dolphin, 2013). Cavα2δ C-terminus contains a hydrophobic domain that is predicted to be a helical trans-membrane segment (Calderón-Rivera et al., 2012). However, this would leave a very short intracellular sequence, particularly in the case of the Cavα2δ4 subunit (only a single amino acid). Alternatively, Cavα2δ might be glycosyl-phosphatidylinositol (GPI)-anchored (Davies et al., 2010). The α2 peptide contains protein domains including a von Willebrand factor A (VWA) domain generally involved in protein–protein interactions and a Ca^{2+} channels-chemotaxis receptor (cache) domain also found in bacterial chemosensing proteins. While the function of the VWA domain has been partially identified by mutating its metal ion-dependent adhesion motif (MIDAS), the functional role of the cache domain is unknown (Dolphin, 2012). On the basis of the predicted cDNA sequences (Genbank: XM_003251054, XM_003251053 and XM_623846), we cloned and arbitrarily numbered three *A. mellifera* Cavα2δ subunits. None of these sequences showed high homology with a specific mammalian Cavα2δ subunit (Table 2). The genomic sequences of AmelCavα2δ1, α2δ2 and α2δ3 contain 17, 12 and 22 exons, respectively, that are predicted to span 9–10 kb (Supplementary Fig. 3). AmelCavα2δ1, AmelCavα2δ2 and AmelCavα2δ3 cDNAs (deposited in Genbank under the numbers KJ485707, KJ485708 and KJ485709) encode proteins of 1204, 1198 and 1193 amino acids, respectively (Fig. 8). We did not find any evidence for the existence of alternative exons for any of the three Cavα2δ subunits. All Cavα2δ subunits contain a signal peptide at the N-terminus, in agreement with their predicted exofacial N-terminus, and a hydrophobic domain at the C-terminus (Fig. 8). If this hydrophobic domain was a trans-membrane segment then the cytoplasmic C-terminus of AmelCava2δ1 would be 5-amino acid long, whereas that of AmelCava2δ2 and AmelCava2δ3 would be non-existent (Fig. 8). To assess whether the honeybee Cavα2δ subunits could be GPI-anchored proteins like some of the mammalian Cavα2δ subunits (Robinson et al., 2011), we analyzed their sequences using three independent algorithms: Big-PI (Eisenhaber et al., 1999), FragAnchor (Poisson

Table 2
Sequence homology between honeybee and human Cavα2δ subunits.

% Amino acid identity	HsapCavα2δ1	HsapCavα2δ2	HsapCavα2δ3	HsapCavα2δ4
AmelCavα2δ1	23	22	31	29
AmelCavα2δ2	23	24	28	29
AmelCavα2δ3	22	22	29	30

Genbank Accession number of the human (Hsap) subunits: Cavα2δ1 (NP_000713), Cavα2δ2 (NP_006021), Cavα2δ3 (NP_060868) and Cavα2δ4 (NP_758952).

Fig. 8. Alignment of the amino acid sequences of the three AmelCavα2δ subunits. Dashes represent gaps introduced to maximize sequence alignment. The signal peptide at the N-terminus (*italic*) and the trans-membrane segment at the C-terminus (**bold**) were predicted with SignalP4.0 and TMbase on the Expasy server (www.expasy.org), respectively. The VWA domain, which includes the MIDAS site (*), is underlined. The two cysteines residues involved in the formation of the disulfide bond in mammalian Cavα2δ1 are marked (#). The potential GPI-anchor sites C1170 and K1168 (ω) were identified with bigPI and PredGPI, respectively. Sequences were deposited in Genbank (accession numbers KJ485707–KJ485709).

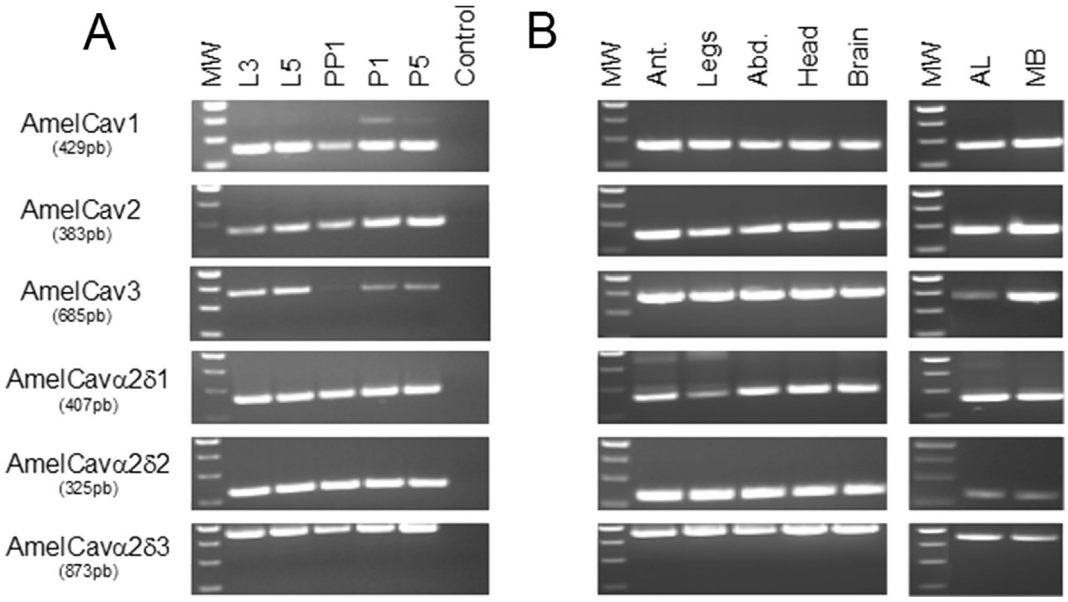

Fig. 9. Developmental and tissue specific expression of the AmelCavα and AmelCavα2δ subunits. Total RNA was extracted from whole honeybees at different developmental stages: larva (L3 and L5), pre-pupa (PP1) and pupa (P1 and P5) (**A**), or from adult tissues: antenna (Ant.), legs, abdomen (Abd.), head, brain, antennal lobes (AL) and mushroom bodies (MB) (**B**). Note that there is a faint band of the expected size for AmelCav3 at the PP1 stage.

et al., 2007) and PredGPI (Pierleoni et al., 2008). The three programs (Supplementary Table 2) predicted that AmelCavα2δ1 was not GPI-anchored and that AmelCavα2δ3 is GPI-anchored, but the site of post-translational modification predicted by Big-PI is different from the one predicted by PredGPI (both indicated by ω in Fig. 8). Conversely, only two programs predicted that AmelCavα2δ2 was GPI-anchored. Similar discrepancies were also reported for the mammalian Cavα2δ subunits (Robinson et al., 2011).

3.5. Expression of Ca^{2+} channel subunits during development and in adult honeybees

To evaluate the physiological functions of Ca^{2+} channels in honeybees, we first checked the expression of the different subunits during development and in different tissues from adult bees by RT-PCR (Fig. 9). The three AmelCavα and the three AmelCavα2δ subunits were expressed from the larval stage and throughout development, suggesting that Ca^{2+} channels may be involved in bee pre-imaginal development. Compared to the different subunits, AmelCav3 varied most during development, but this needs to be more precisely assessed. All subunits were also expressed in all adult tissues assessed, including legs and brain, and more precisely, they were all expressed in sub-regions of the brain namely the antennal lobes and the mushroom bodies. Knowing the central role of Ca^{2+} signaling in multiple cellular functions, the ubiquitous expression of all honeybee Ca^{2+} channel subunits is not surprising.

3.6. Functional expression of the honeybee Ca^{2+} channels

To our knowledge, Ca^{2+} currents resulting from the expression of insect Ca^{2+} channel subunits in a heterologous expression system have never been recorded. This could be due to the lack of one or more auxiliary subunits in previous experiments, as reported for squid Ca^{2+} channels (Kimura and Kubo, 2002). We therefore injected in *Xenopus* oocytes a mixture of *in vitro* transcribed RNAs encoding AmelCav1a or AmelCav2a together with those encoding AmelCavβc and AmelCavα2δ1 (Fig. 10). Even in these conditions, however, the expression of Ca^{2+} currents was rarely observed and frequently we did not record any current at all in a whole batch of injected oocytes. This may suggest the existence of RNA secondary structure, post-translational modifications or unknown regulatory subunits that could chaperone Ca^{2+} channels to the plasma membrane. We obtained similar results by combining other honeybee Cavβ and Cavα2δ subunits (not shown). Nevertheless, we could draw current–voltage curves for both AmelCav1a and AmelCav2a channels that clearly displayed distinct properties (Table 3). On the other hand, expression of AmelCav3a alone gave more reliable results. Compared to AmelCav1a and AmelCav2a, this channel was clearly transient with the fast inactivation kinetics described for mammalian Cav3 channels (Fig. 10A). This channel activated at around −50 mV and showed a more negative reversal potential than AmelCav1a and AmelCav2a channels (Fig. 10B and Table 3). We unambiguously conclude that AmelCav3 encodes a LVA Ca^{2+} channel. Nevertheless, improving the expression of these channels would be advantageous for a more complete characterization of their electrophysiological and pharmacological properties.

In conclusion, we have characterized all the voltage-gated Ca^{2+} channel subunits of the honeybee *A. mellifera*. They include functionally important protein domains identified in mammalian subunits. When expressed in *Xenopus* oocytes, they produce Ca^{2+} channels with distinctive properties. The availability of these subunits opens new opportunities for elucidating the role of Ca^{2+} channels in honeybee physiology.

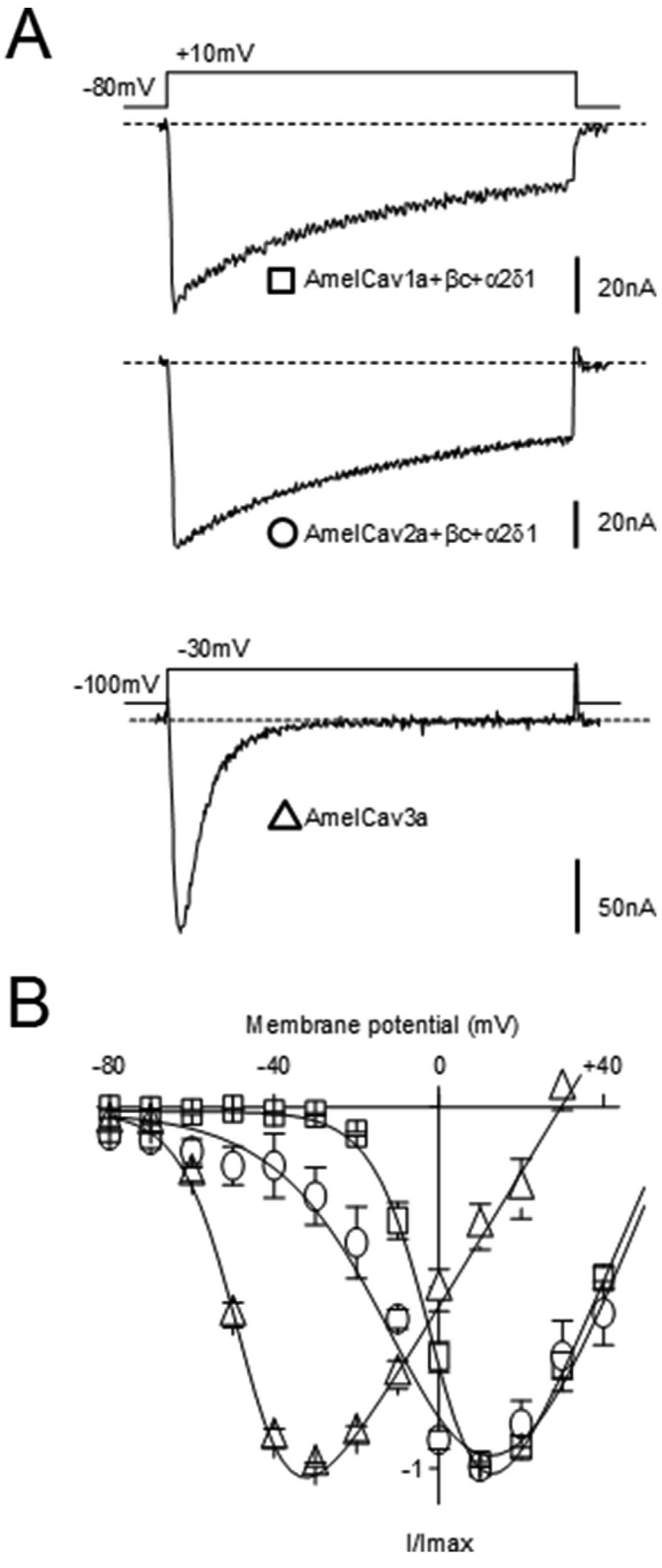

Fig. 10. Recordings of honeybee Ca^{2+} channel currents. **A**. Traces of currents obtained in *Xenopus* oocytes injected with a mixture of *in vitro* transcribed AmelCav1a (square) or AmelCav2a (circle) together with AmelCavβc and AmelCavα2δ1, or AmelCav3a (triangle) RNAs. **B**. Current–voltage relationships obtained with the three subunit combinations. Note the fast inactivation and the hyperpolarizing shift of the current–voltage curve obtained with AmelCav3.

Table 3
Parameters of the current–voltage curves obtained for honeybee Ca^{2+} channels.

	Va (mV)	k (mV)	Erev (mV)	n
AmelCav1a	5 ± 2	8.8 ± 0.9	56 ± 2	4
AmelCav2a	4 ± 6	14.2 ± 1.7	54 ± 5	3
AmelCav3a	46 ± 1	7.0 ± 0.4	26 ± 1	8

Va: potential for half activation, k: slope factor, Erev: reversal potential.

Acknowledgments

This work was supported by « Centre National de la Recherche Scientifique (CNRS) », « Institut National de la Santé et de la Recherche Médicale (INSERM) », « Institut National de la Recherche Agronomique (INRA) » and funded by « Agence Nationale pour la Recherche (NR-13-BSV7-0010, Bee-channel) ». The authors wish to thank the beekeepers and people who collected bee specimens without whom this work would not have been possible.

Appendix A. Supplementary data

Supplementary data related to this article can be found at http://dx.doi.org/10.1016/j.ibmb.2015.01.005.

References

Andrade, A., Sandoval, A., Oviedo, N., De Waard, M., Elias, D., Felix, R., 2007. Proteolytic cleavage of the voltage-gated Ca^{2+} channel alpha2delta subunit: structural and functional features. Eur. J. Neurosci. 25, 1705–1710. http://dx.doi.org/10.1111/j.1460-9568.2007.05454.x.

Bellis, M., Cens, T., Charnet, P., Rousset, M., 2013. Voltage-gated Ca^{2+} channels signalling to the nucleus. In: Stephens, G., Mochida, S. (Eds.), Modulation of Presynaptic Calcium Channels. Springer, Netherlands, Dordrecht, pp. 175–198. http://dx.doi.org/10.1007/978-94-007-6334-0.

Bezanilla, F., 2008. How membrane proteins sense voltage. Nat. Rev. Mol. Cell Biol. 9, 323–332. http://dx.doi.org/10.1038/nrm2376.

Bouchard, C., Price, R.B., Moneypenny, C.G., Thompson, L.F., Zillhardt, M., Stalheim, L., Anderson, P.A.V., 2006. Cloning and functional expression of voltage-gated ion channel subunits from cnidocytes of the Portuguese Man O'War Physalia physalis. J. Exp. Biol. 209, 2979–2989. http://dx.doi.org/10.1242/jeb.02314.

Bourinet, E., Soong, T.W., Sutton, K., Slaymaker, S., Mathews, E., Monteil, A., Zamponi, G.W., Nargeot, J., Snutch, T.P., 1999. Splicing of alpha 1A subunit gene generates phenotypic variants of P- and Q-type calcium channels. Nat. Neurosci. 2, 407–415. http://dx.doi.org/10.1038/8070.

Buraei, Z., Yang, J., 2010. The ß subunit of voltage-gated Ca^{2+} channels. Physiol. Rev. 90, 1461–1506. http://dx.doi.org/10.1152/physrev.00057.2009.

Butland, S.L., Devon, R.S., Huang, Y., Mead, C.-L., Meynert, A.M., Neal, S.J., Lee, S. Sen, Wilkinson, A., Yang, G.S., Yuen, M.M.S., Hayden, M.R., Holt, R.A., Leavitt, B.R., Ouellette, B.F.F., 2007. CAG-encoded polyglutamine length polymorphism in the human genome. BMC Genomics 8, 126. http://dx.doi.org/10.1186/1471-2164-8-126.

Calderón-Rivera, A., Andrade, A., Hernández-Hernández, O., González-Ramírez, R., Sandoval, A., Rivera, M., Gomora, J.C., Felix, R., 2012. Identification of a disulfide bridge essential for structure and function of the voltage-gated Ca(2+) channel α(2)δ-1 auxiliary subunit. Cell Calcium 51, 22–30. http://dx.doi.org/10.1016/j.ceca.2011.10.002.

Catterall, W.A., 2011. Voltage-gated calcium channels. Cold Spring Harb. Perspect. Biol. 3, a003947. http://dx.doi.org/10.1101/cshperspect.a003947.

Cens, T., Mangoni, M.E., Nargeot, J., Charnet, P., 1996. Modulation of the α1A Ca^{2+} channel by β subunits at physiological Ca^{2+} concentration. FEBS Lett. 391, 232–237. http://dx.doi.org/10.1016/0014-5793(96)00704-1.

Cens, T., Restituito, S., Charnet, P., 1999. Regulation of Ca-sensitive inactivation of a L-type Ca^{2+} channel by specific domains of beta subunits. FEBS Lett. 450, 17–22. http://dx.doi.org/10.1016/S0014-5793(99)00463-9.

Cens, T., Rousset, M., Charnet, P., 2011. Two sets of amino acids of the domain I of Cav2.3 Ca(2+) channels contribute to their high sensitivity to extracellular protons. Pflüg. Arch. Eur. J. Physiol. 462, 303–314. http://dx.doi.org/10.1007/s00424-011-0974-x.

Cens, T., Rousset, M., Collet, C., Raymond, V., Démares, F., Quintavalle, A., Bellis, M., Le Conte, Y., Chahine, M., Charnet, P., 2013. Characterization of the first honeybee Ca^{2+} channel subunit reveals two novel species- and splicing-specific modes of regulation of channel inactivation. Pflüg. Arch. Eur. J. Physiol. 465, 985–996. http://dx.doi.org/10.1007/s00424-013-1223-2.

Cens, T., Rousset, M., Kajava, A., Charnet, P., 2007. Molecular determinant for specific Ca/Ba selectivity profiles of low and high threshold Ca^{2+} channels. J. Gen. Physiol. 130, 415–425. http://dx.doi.org/10.1085/jgp.200709771.

Cens, T., Rousset, M., Leyris, J.-P., Fesquet, P., Charnet, P., 2006. Voltage- and calcium-dependent inactivation in high voltage-gated Ca(2+) channels. Prog. Biophys. Mol. Biol. 90, 104–117. http://dx.doi.org/10.1016/j.pbiomolbio.2005.05.013.

Chen, Y.-H., Li, M.-H., Zhang, Y., He, L.-L., Yamada, Y., Fitzmaurice, A., Shen, Y., Zhang, H., Tong, L., Yang, J., 2004. Structural basis of the alpha1-beta subunit interaction of voltage-gated Ca^{2+} channels. Nature 429, 675–680. http://dx.doi.org/10.1038/nature02641.

Collet, C., 2009. Excitation-contraction coupling in skeletal muscle fibers from adult domestic honeybee. Pflüg. Arch. Eur. J. Physiol. 458, 601–612. http://dx.doi.org/10.1007/s00424-009-0642-6.

Davies, A., Kadurin, I., Alvarez-Laviada, A., Douglas, L., Nieto-Rostro, M., Bauer, C.S., Pratt, W.S., Dolphin, A.C., 2010. The alpha2delta subunits of voltage-gated calcium channels form GPI-anchored proteins, a posttranslational modification essential for function. Proc. Natl. Acad. Sci. U. S. A. 107, 1654–1659. http://dx.doi.org/10.1073/pnas.0908735107.

Dawson, T.F., Boone, A.N., Senatore, A., Piticaru, J., Thiyagalingam, S., Jackson, D., Davison, A., Spafford, J.D., 2014. Gene splicing of an invertebrate beta subunit (LCavβ) in the N-terminal and HOOK domains and its regulation of LCav1 and LCav2 calcium channels. PLoS One 9, e92941. http://dx.doi.org/10.1371/journal.pone.0092941.

Dereeper, A., Guignon, V., Blanc, G., Audic, S., Buffet, S., Chevenet, F., Dufayard, J.F., Guindon, S., Lefort, V., Lescot, M., Claverie, J.M., Gascuel, O., 2008. Phylogeny.fr: robust phylogenetic analysis for the non-specialist. Nucleic Acids Res. 36, W465–W469. http://dx.doi.org/10.1093/nar/gkn180.

Dolphin, A.C., 2012. Calcium channel auxiliary alpha(2)delta and beta subunits: trafficking and one step beyond. Nat. Rev. Neurosci. 13, 542–555. http://dx.doi.org/10.1038/nrn3311.

Dolphin, A.C., 2013. The α2δ subunits of voltage-gated calcium channels. Biochim. Biophys. Acta 1828, 1541–1549. http://dx.doi.org/10.1016/j.bbamem.2012.11.019.

Eisenhaber, B., Bork, P., Eisenhaber, F., 1999. Prediction of potential GPI-modification sites in proprotein sequences. J. Mol. Biol. 292, 741–758. http://dx.doi.org/10.1006/jmbi.1999.3069.

Elsik, C.G., Worley, K.C., Bennett, A.K., Beye, M., Camara, F., Childers, C.P., de Graaf, D.C., Debyser, G., Deng, J., Devreese, B., Elhaik, E., Evans, J.D., Foster, L.J., Graur, D., Guigo, R., Hoff, K.J., Holder, M.E., Hudson, M.E., Hunt, G.J., Jiang, H., Joshi, V., Khetani, R.S., Kosarev, P., Kovar, C.L., Ma, J., Maleszka, R., Moritz, R.F.A., Munoz-Torres, M.C., Murphy, T.D., Muzny, D.M., Newsham, I.F., Reese, J.T., Robertson, H.M., Robinson, G.E., Rueppell, O., Solovyev, V., Stanke, M., Stolle, E., Tsuruda, J.M., Vaerenbergh, M. Van, Waterhouse, R.M., Weaver, D.B., Whitfield, C.W., Wu, Y., Zdobnov, E.M., Zhang, L., Zhu, D., Gibbs, R.A., 2014. Finding the missing honey bee genes: lessons learned from a genome upgrade. BMC Genomics 15, 86. http://dx.doi.org/10.1186/1471-2164-15-86.

Felix, R., Calderón-Rivera, A., Andrade, A., 2013. Regulation of high voltage activated Ca^{2+} channel function, trafficking, and membrane stability by auxiliary subunits. WIRES Memb. Transp. Signal. 2, 207–220. http://dx.doi.org/10.1002/wmts.93.

Gatchel, J.R., Zoghbi, H.Y., 2005. Diseases of unstable repeat expansion: mechanisms and common principles. Nat. Rev. Genet. 6, 743–755. http://dx.doi.org/10.1038/nrg1691.

Hanlon, M.R., Berrow, N.S., Dolphin, A.C., Wallace, B.A., 1999. Modelling of a voltage-dependent Ca^{2+} channel beta subunit as a basis for understanding its functional properties. FEBS Lett. 445, 366–370. http://dx.doi.org/10.1016/S0014-5793(99)00156-8.

Hans, M., Urrutia, A., Deal, C., Brust, P.F., Stauderman, K., Ellis, S.B., Harpold, M.M., Johnson, E.C., Williams, M.E., 1999. Structural elements in domain IV that influence biophysical and pharmacological properties of human alpha1A-containing high-voltage-activated calcium channels. Biophys. J. 76, 1384–1400. http://dx.doi.org/10.1016/S0006-3495(99)77300-5.

He, L.-L., Zhang, Y., Chen, Y.-H., Yamada, Y., Yang, J., 2007. Functional modularity of the beta-subunit of voltage-gated Ca^{2+} channels. Biophys. J. 93, 834–845. http://dx.doi.org/10.1529/biophysj.106.101691.

Jeziorski, M.C., Greenberg, R.M., Anderson, P.A., 2000. The molecular biology of invertebrate voltage-gated Ca(2+) channels. J. Exp. Biol. 203, 841–856.

Jeziorski, M.C., Greenberg, R.M., Clark, K.S., Anderson, P.A., 1998. Cloning and functional expression of a voltage-gated calcium channel alpha1 subunit from jellyfish. J. Biol. Chem. 273, 22792–22799. http://dx.doi.org/10.1074/jbc.273.35.22792.

Kang, H.-W., Park, J.-Y., Jeong, S.-W., Kim, J.-A., Moon, H.-J., Perez-Reyes, E., Lee, J.-H., 2006. A molecular determinant of nickel inhibition in Cav3.2 T-type calcium channels. J. Biol. Chem. 281, 4823–4830. http://dx.doi.org/10.1074/jbc.M510197200.

Kimura, T., Kubo, T., 2002. Functional identification of a cloned squid presynaptic voltage-dependent calcium channel. Neuroreport 13, 2389–2393. http://dx.doi.org/10.1097/01.wnr.0000048022.74602.29.

Kimura, T., Kubo, T., 2003. Cloning and functional characterization of squid voltage-dependent Ca^{2+} channel β subunits: involvement of N-terminal sequences in differential modulation of the current. Neurosci. Res. 46, 105–117. http://dx.doi.org/10.1016/S0168-0102(03)00038-5.

Kloppenburg, P., Kirchhof, B.S., Mercer, A.R., 1999. Voltage-activated currents from adult honeybee (*Apis mellifera*) antennal motor neurons recorded in vitro and in situ. J. Neurophysiol. 81, 39–48.

Kohn, A.B., Anderson, P.A., Roberts-Misterly, J.M., Greenberg, R.M., 2001. Schistosome calcium channel beta subunits. Unusual modulatory effects and potential role in the action of the antischistosomal drug praziquantel. J. Biol. Chem. 276, 36873–36876. http://dx.doi.org/10.1074/jbc.C100273200.

Laurent, S., Masson, C., Jakob, I., 2002. Whole-cell recording from honeybee olfactory receptor neurons: ionic currents, membrane excitability and odourant response in developing workerbee and drone. Eur. J. Neurosci. 15, 1139–1152. http://dx.doi.org/10.1046/j.1460-9568.2002.01954.x.

Lee, A., Westenbroek, R.E., Haeseleer, F., Palczewski, K., Scheuer, T., Catterall, W.A., 2002. Differential modulation of Ca(v)2.1 channels by calmodulin and Ca^{2+}-binding protein 1. Nat. Neurosci. 5, 210–217. http://dx.doi.org/10.1038/nn805.

Miranda-Laferte, E., Schmidt, S., Jara, A.C., Neely, A., Hidalgo, P., 2012. A short polybasic segment between the two conserved domains of the β2a-subunit modulates the rate of inactivation of R-type calcium channel. J. Biol. Chem. 287, 32588–32597. http://dx.doi.org/10.1074/jbc.M112.362509.

Olcese, R., Qin, N., Schneider, T., Neely, A., Wei, X., Stefani, E., Birnbaumer, L., 1994. The amino terminus of a calcium channel β subunit sets rates of channel inactivation independently of the subunit's effect on activation. Neuron 13, 1433–1438. http://dx.doi.org/10.1016/0896-6273(94)90428-6.

Opatowsky, Y., Chen, C.-C., Campbell, K.P., Hirsch, J.A., 2004. Structural analysis of the voltage-dependent calcium channel beta subunit functional core and its complex with the alpha 1 interaction domain. Neuron 42, 387–399. http://dx.doi.org/10.1016/S0896-6273(04)00250-8.

Pierleoni, A., Martelli, P.L., Casadio, R., 2008. PredGPI: a GPI-anchor predictor. BMC Bioinform. 9, 392. http://dx.doi.org/10.1186/1471-2105-9-392.

Poisson, G., Chauve, C., Chen, X., Bergeron, A., 2007. FragAnchor: a large-scale predictor of glycosylphosphatidylinositol anchors in eukaryote protein sequences by qualitative scoring. Genomics Proteomics Bioinform. 5, 121–130. http://dx.doi.org/10.1016/S1672-0229(07)60022-9.

Qin, N., Olcese, R., Zhou, J., Cabello, O.A., Birnbaumer, L., Stefani, E., 1996. Identification of a second region of the beta-subunit involved in regulation of calcium channel inactivation. Am. J. Physiol. 271, C1539–C1545.

Restituito, S., Cens, T., Barrere, C., Geib, S., Galas, S., De Waard, M., Charnet, P., 2000. The [beta]2a subunit is a molecular groom for the Ca^{2+} channel inactivation gate. J. Neurosci. 20, 9046–9052.

Richards, M.W., Leroy, J., Pratt, W.S., Dolphin, A.C., 2007. The HOOK-domain between the SH3 and the GK domains of Cavbeta subunits contains key determinants controlling calcium channel inactivation. Channels 1, 92–101. http://dx.doi.org/10.4161/chan.4145.

Robinson, P., Etheridge, S., Song, L., Shah, R., Fitzgerald, E.M., Jones, O.T., 2011. Targeting of voltage-gated calcium channel α2δ-1 subunit to lipid rafts is independent from a GPI-anchoring motif. PLoS One 6, e19802. http://dx.doi.org/10.1371/journal.pone.0019802.

Ryglewski, S., Lance, K., Levine, R.B., Duch, C., 2012. Ca(v)2 channels mediate low and high voltage-activated calcium currents in Drosophila motoneurons. J. Physiol. 590, 809–825. http://dx.doi.org/10.1113/jphysiol.2011.222836.

Salvador-Recatalà, V., Greenberg, R.M., 2012. Calcium channels of schistosomes: unresolved questions and unexpected answers. WIRES Memb. Transp. Signal 1, 85–93. http://dx.doi.org/10.1002/wmts.19.

Sandoz, J.C., 2011. Behavioral and neurophysiological study of olfactory perception and learning in honeybees. Front. Syst. Neurosci. 5, 98. http://dx.doi.org/10.3389/fnsys.2011.00098.

Sather, W.A., McCleskey, E.W., 2003. Permeation and selectivity in calcium channels. Annu. Rev. Physiol. 65, 133–159. http://dx.doi.org/10.1016/S0006-3495(01)76007-9.

Schäfer, S., Rosenboom, H., Menzel, R., 1994. Ionic currents of Kenyon cells from the mushroom body of the honeybee. J. Neurosci. 14, 4600–4612.

Senatore, A., Spafford, J.D., 2010. Transient and big are key features of an invertebrate T-type channel (LCav3) from the central nervous system of Lymnaea stagnalis. J. Biol. Chem. 285, 7447–7458. http://dx.doi.org/10.1074/jbc.M109.090753.

Smith, L.A., Peixoto, A.A., Kramer, E.M., Villella, A., Hall, J.C., 1998. Courtship and visual defects of cacophony mutants reveal functional complexity of a calcium-channel alpha1 subunit in Drosophila. Genetics 149, 1407–1426.

Spafford, J.D., Chen, L., Feng, Z.-P., Smit, A.B., Zamponi, G.W., 2003. Expression and modulation of an invertebrate presynaptic calcium channel alpha1 subunit homolog. J. Biol. Chem. 278, 21178–21187. http://dx.doi.org/10.1074/jbc.M302212200.

Spafford, J.D., Dunn, T., Smit, A.B., Syed, N.I., Zamponi, G.W., 2006. In vitro characterization of L-type calcium channels and their contribution to firing behavior in invertebrate respiratory neurons. J. Neurophysiol. 95, 42–52. http://dx.doi.org/10.1152/jn.00658.2005.

Taiakina, V., Boone, A.N., Fux, J., Senatore, A., Weber-Adrian, D., Guillemette, J.G., Spafford, J.D., 2013. The calmodulin-binding, short linear motif, NSCaTE is conserved in L-type channel ancestors of vertebrate Cav1.2 and Cav1.3 channels. PLoS One 8, e61765. http://dx.doi.org/10.1371/journal.pone.0061765.

Tombola, F., Pathak, M.M., Isacoff, E.Y., 2006. How does voltage open an ion channel? Annu. Rev. Cell. Dev. Biol. 22, 23–52. http://dx.doi.org/10.1146/annurev.cellbio.21.020404.145837.

Tyson, J.R., Snutch, T.P., 2013. Molecular nature of voltage-gated calcium channels: structure and species comparison. WIRES Memb. Transp. Signal 2, 181–206. http://dx.doi.org/10.1002/wmts.91.

Van Petegem, F., Clark, K.A., Chatelain, F.C., Minor, D.L., 2004. Structure of a complex between a voltage-gated calcium channel beta-subunit and an alpha-subunit domain. Nature 429, 671–675. http://dx.doi.org/10.1038/nature02588.

Venkatachalan, S.P., Bushman, J.D., Mercado, J.L., Sancar, F., Christopherson, K.R., Boileau, A.J., 2007. Optimized expression vector for ion channel studies in

Xenopus oocytes and mammalian cells using alfalfa mosaic virus. Pflug. Arch. Eur. J. Physiol. 454, 155–163. http://dx.doi.org/10.1007/s00424-006-0183-1.

Vitko, I., Bidaud, I., Arias, J.M., Mezghrani, A., Lory, P., Perez-Reyes, E., 2007. The I-II loop controls plasma membrane expression and gating of Ca(v)3.2 T-type Ca^{2+} channels: a paradigm for childhood absence epilepsy mutations. J. Neurosci. 27, 322–330. http://dx.doi.org/10.1523/JNEUROSCI.1817-06.2007.

Weinstock, G.M., Robinson, G.E., Gibbs, R.A., Worley, K.C., Evans, J.D., Maleszka, R., Robertson, H.M., Weaver, D.B., Beye, M., Bork, P., Elsik, C.G., Hartfelder, K., Hunt, G.J., Zdobnov, E.M., Amdam, G.V., Bitondi, M.M.G., Collins, A.M., Cristino, A.S., Michael, H., Lattorff, G., Lobo, C.H., Moritz, R.F.A., Nunes, F.M.F., Page, R.E., Simes, Z.L.P., Wheeler, D., Carninci, P., Fukuda, S., Hayashizaki, Y., Kai, C., Kawai, J., Sakazume, N., Sasaki, D., Tagami, M., Albert, S., Baggerman, G., Beggs, K.T., Bloch, G., Cazzamali, G., Cohen, M., Drapeau, M.D., Eisenhardt, D., Emore, C., Ewing, M.A., Fahrbach, S.E., Fort, S., Grimmelikhuijzen, C.J.P., Hauser, F., Hummon, A.B., Huybrechts, J., Jones, A.K., Kadowaki, T., Kaplan, N., Kucharski, R., Leboulle, G., Linial, M., Littleton, J.T., Mercer, A.R., Richmond, T.A., RodriguezZas, S.L., Rubin, E.B., Sattelle, D.B., Schlipalius, D., Schoofs, L., Shemesh, Y., Sweedler, J.V., Velarde, R., Verleyen, P., Vierstraete, E., Williamson, M.R., Ament, S.A., Brown, S.J., Corona, M., Dearden, P.K., Dunn, W.A., Elekonich, M.M., Fujiyuki, T., Gattermeier, I., Gempe, T., Hasselmann, M., Kage, E., Kamikouchi, A., Kubo, T., Kunieda, T., Lorenzen, M., Milshina, N.V., Morioka, M., Ohashi, K., Overbeek, R., Ross, C.A., Schioett, M., Shippy, T., Takeuchi, H., Toth, A.L., Willis, J.H., Wilson, M.J., Gordon, K.H.J., Letunic, I., Hackett, K., Peterson, J., Felsenfeld, A., Guyer, M., Solignac, M., Agarwala, R., Cornuet, J.M., Monnerot, M., Mougel, F., Reese, J.T., Vautrin, D., Gillespie, J.J., Cannone, J.J., Gutell, R.R., Johnston, J.S., Eisen, M.B., Iyer, V.N., Iyer, V., Kosarev, P., Mackey, A.J., Solovyev, V., Souvorov, A., Aronstein, K.A., Bilikova, K., Chen, Y.P., Clark, A.G., Decanini, L.I., Gelbart, W.M., Hetru, C., Hultmark, D., Imler, J.-L., Jiang, H., Kanost, M., Kimura, K., Lazzaro, B.P., Lopez, D.L., Simuth, J., Thompson, G.J., Zou, Z., De Jong, P., Sodergren, E., Csürös, M., Milosavljevic, A., Osoegawa, K., Richards, S., Shu, C.-L., Duret, L., Elhaik, E., Graur, D., Anzola, J.M., Campbell, K.S., Childs, K.L., Collinge, D., Crosby, M.A., Dickens, C.M., Grametes, L.S., Grozinger, C.M., Jones, P.L., Jorda, M., Ling, X., Matthews, B.B., Miller, J., Mizzen, C., Peinado, M.A., Reid, J.G., Russo, S.M., Schroeder, A.J., St Pierre, S.E., Wang, Y., Zhou, P., Jiang, H., Kitts, P., Ruef, B., Venkatraman, A., Zhang, L., Aquino-Perez, G., Whitfield, C.W., Behura, S.K., Berlocher, S.H., Sheppard, W.S., Smith, D.R., Suarez, A.V., Tsutsui, N.D., Wei, X., Wheeler, D., Havlak, P., Li, B., Liu, Y., Jolivet, A., Lee, S., Nazareth, L.V., Pu, L.-L., Thorn, R., Stolc, V., Newman, T., Samanta, M., Tongprasit, W.A., Claudianos, C., Berenbaum, M.R., Biswas, S., de Graaf, D.C., Feyereisen, R., Johnson, R.M., Oakeshott, J.G., Ranson, H., Schuler, M.A., Muzny, D., Chacko, J., Davis, C., Dinh, H., Gill, R., Hernandez, J., Hines, S., Hume, J., Jackson, L., Kovar, C., Lewis, L., Miner, G., Morgan, M., Nguyen, N., Okwuonu, G., Paul, H., Santibanez, J., Savery, G., Svatek, A., Villasana, D., Wright, R., 2006. Insights into social insects from the genome of the honeybee *Apis mellifera*. Nature. http://dx.doi.org/10.1038/nature05260.

Williams, A.J., Paulson, H.L., 2008. Polyglutamine neurodegeneration: protein misfolding revisited. Trends Neurosci. 31, 521–528. http://dx.doi.org/10.1016/j.tins.2008.07.004.

Zheng, W., Feng, G., Ren, D., Eberl, D.F., Hannan, F., Dubald, M., Hall, L.M., 1995. Cloning and characterization of a calcium channel alpha 1 subunit from Drosophila melanogaster with similarity to the rat brain type D isoform. J. Neurosci. 15, 1132–1143.